Am J Transl Res 2025;17(7):5625-5640
www.ajtr.org /ISSN:1943-8141/AJTR0165730

Original Article

Development of a carbon nanoparticle-guided nomogram for predicting lateral cervical lymph node metastasis in clinically node-negative papillary thyroid carcinoma

Hui Qu, Pisong Li, Hongbo Qu, Xiaoyu Zhu, Zhongbin Han, Hongshen Chen

Department of Breast and Thyroid Surgery, Affiliated Zhongshan Hospital of Dalian University, Dalian 116001, Liaoning, The People's Republic of China

Received April 29, 2025; Accepted July 4, 2025; Epub July 25, 2025; Published July 30, 2025

Abstract: Objective: To develop and validate a carbon nanoparticle-enhanced nomogram for predicting lateral lymph node (LLN) metastasis in patients with clinically node-negative (cN0) papillary thyroid carcinoma (PTC). Methods: A retrospective analysis was conducted on 421 cN0 PTC patients treated between 2014 and 2020. Patients were randomly divided into training (n=316) and internal validation (n=105) cohorts. Least absolute shrinkage and selection operator (LASSO) regression and Cox regression analyses were performed to identify predictive factors from clinical, ultrasonographic, and carbon nanoparticle tracing data. Model performance was evaluated using receiver operating characteristic (ROC) curves, calibration plots, and decision curve analysis (DCA). Results: Independent predictors identified included age (HR: 0.944, 95% CI: 0.908-0.982), tumor diameter ≥1 cm (HR: 0.221, 95% CI: 0.053-1.920), regular tumor morphology (HR: 0.090, 95% CI: 0.020-0.470), and the number of carbon nanoparticle-stained positive lateral lymph nodes (HR: 0.000, 95% CI: 0.000-0.231). The nomogram showed excellent discrimination, with an AUC of 0.911 in the training set and 0.916 in the validation set, and good calibration (Brier scores of 5.70 and 4.50, respectively). DCA confirmed the clinical utility of the model across a range of risk thresholds. Conclusion: This carbon nanoparticle-guided nomogram is a practical and highly accurate tool for intraoperative risk stratification of LLN metastasis in cN0 PTC patients. Integrating tracer-based lymph node assessment with conventional clinicopathological factors enhances predictive capability compared to existing methods, potentially reducing unnecessary neck dissections while ensuring appropriate management of high-risk cases. Multicenter validation and incorporation of molecular markers are important next steps toward clinical implementation.

Keywords: Papillary thyroid carcinoma, lateral cervical lymph node metastasis, prediction model, independent predictors

Introduction

Thyroid cancer (TC) is the most common malignancy of the endocrine system, and its incidence has risen significantly around the world in recent years, now accounting for approximately 30% of all endocrine malignancies [1]. About 85-90% of TC cases are papillary thyroid carcinoma (PTC), which is the most prevalent histological subtype [2]. Despite its generally excellent prognosis, with a 10-year survival rate exceeding 90% [3], lymph node metastasis (LNM) significantly affects long-term outcomes and increases the risk of recurrence. The most common pattern is central lymph node (CLN) metastasis, which has a high incidence but generally favorable prognosis [4]. The second most common pattern is lateral lymph node (LLN) metastasis, occurring in 10-40% of PTC patients [5]. Due to its association with higher recurrence rates and poorer survival, LLN metastasis is a major prognostic factor [6]. However, accurately predicting the risk of LLN metastasis using preoperative tests remains challenging. Even patients with clinically node-negative (cN0) PTC still face a considerable risk of occult metastasis [7]. This diagnostic uncertainty continues to generate controversy regarding the optimal management of potential LLN metastasis in cN0 PTC cases.

Given the difficulty of detecting occult LLN metastasis - which may affect 30% to 60% of

https://doi.org/10.62347/JVGT3596

cN0 PTC patients - detailed risk assessment using extensive clinical data is essential [8]. Traditional risk assessment relies on clinicopathological features such as tumor size, extrathyroidal extension, and multifocality; however, these factors alone do not provide sufficient predictive accuracy [9]. Therefore, to overcome current limitations in prediction, more precise risk assessment models are needed. Due to their reliable staining properties, minimal toxicity, and high effectiveness in evaluating LNM, carbon nanoparticles (CNs) have been widely used as lymphatic tracers in radical PTC surgery [10]. A nomogram can integrate multiple clinicopathological and biochemical variables into a visual scoring tool to provide personalized risk estimates [11]. Therefore, the present study aims to develop a comprehensive nomogram that incorporates CN tracing features to predict the likelihood of LLN metastasis in cN0 PTC patients, thereby providing clinicians with a practical tool for individualized decision-making.

Material and methods

Patient population

Based on assumptions from preliminary clinical trials, PASS 15.0 was used to calculate the minimum required sample size. With an estimated LLN metastasis rate of 10% among PTC patients, the following parameters were set: α=0.05, power (1-β) =0.90, and P0=0.9, assuming equal metastasis incidence between the training and validation sets and a training-to-validation ratio of 3:1. The calculated minimum sample size was 129 cases, including at least 96 cases in the training cohort and 33 cases in the validation cohort. After accounting for a 20% attrition rate, the adjusted minimum required sample size was 156 cases (≥116 in the training cohort and ≥40 in the validation cohort).

This retrospective study analyzed 525 patients initially diagnosed with PTC at the Department of Breast and Thyroid Surgery, Affiliated Zhongshan Hospital of Dalian University, between June 2014 and June 2020. LNM status was confirmed by postoperative pathology. Patients were excluded if they had preoperative LLN metastasis (n=23), concurrent malignant tumors (n=32), were over 70 years of age (n=36), had undergone previous thyroidectomy (n=3), or missing clinical data (n=10). Ultimately, 421 patients were included. They were randomly divided into training (n=316) and internal validation (n=105) cohorts at a 3:1 ratio using the random number table method, thus meeting the minimum sample size requirement.

Additionally, an independent cohort of 101 patients meeting the same inclusion criteria between June 2020 and June 2021 was retrospectively enrolled for clinical validation. Based on metastasis status within one year, these patients were stratified into metastatic (n=22) and non-metastatic (n=79) groups to analyze factors associated with metastasis. The complete study enrollment flowchart is shown in **Figure 1**.

This study complied with the World Medical Association's Declaration of Helsinki and relevant Chinese laws and regulations. It was approved by the Ethics Committee of Affiliated Zhongshan Hospital of Dalian University (Approval No.: 2022110). All patient data were obtained under ethical approval from the Department of Breast and Thyroid Surgery, in accordance with institutional review board (IRB) regulations.

Inclusion criteria were: (1) meeting the diagnostic criteria set out in the American Thyroid Association guidelines, with both intraoperative frozen section analysis and postoperative paraffin-embedded pathology confirming PTC [12]; (2) availability of complete clinical data; (3) no preoperative evidence of LLN metastasis; (4) no concurrent malignancies or major organ dysfunction; (5) age between 18-70 years; and (6) undergoing initial thyroidectomy.

Exclusion criteria were: (1) age <18 or >70 years; (2) preoperative confirmation of lateral cervical LNM; (3) major organ dysfunction; (4) other types of thyroid cancer; and (5) psychiatric disorders affecting treatment compliance.

Ultrasonography examination

Ultrasound examinations were performed using Toshiba Aplio 500 and Philips EPIQ 7 systems equipped with linear array probes. The thyroid examination mode was selected to conduct standardized scanning of the thyroid gland and cervical lymph nodes, with evaluation of sonographic characteristics of suspicious lesions.

Research methods

Under ultrasound guidance, 0.2-0.4 mL of CN tracer was aspirated using a 1 mL syringe and

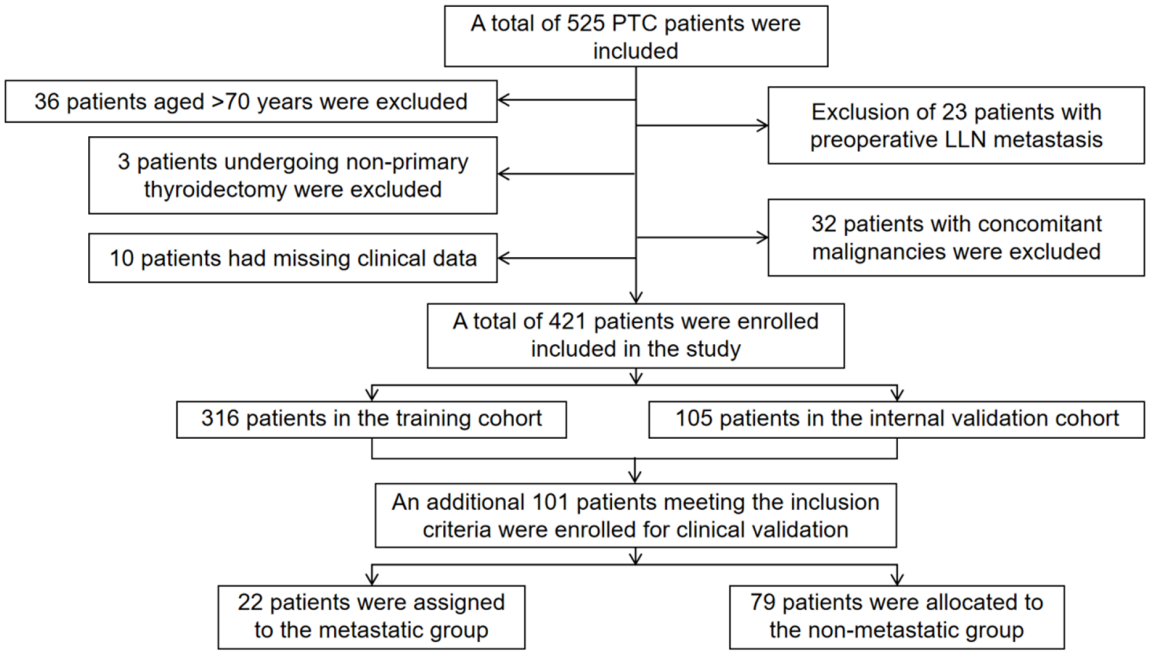

Figure 1. Flow diagram of patient selection steps.

Figure 2. The black-staining pattern in the surgical field following carbon nanoparticles (CNs) injection.

injected obliquely into the thyroid tissue via percutaneous puncture, carefully avoiding tumors and blood vessels. Each thyroid lobe received 1-2 injections of 0.1 mL per site after confirming negative aspiration to prevent intravascular administration. For ultrasonographically suspicious lateral cervical lymph nodes, a minimal volume of tracer could be injected intranodally for intraoperative localization. After injection, the needle was slowly withdrawn with delayed negative-pressure retraction. Patients were instructed to compress the injection site to prevent cutaneous staining or peritissue dispersion of the tracer, which could obscure the surgical field, and to facilitate the intraoperative identification of stained lymph nodes. **Figure 2** shows the black staining of the operative area following CN injection.

Surgical procedures involved a low-collar curvilinear incision, followed by mobilization of the thyroid false capsule to fully expose the gland, allowing meticulous capsular dissection during thyroidectomy. Intraoperative frozen sections confirmed PTC diagnoses in all cases, and mandatory ipsilateral central compartment lymph node dissection was performed. Suspicious carbon-stained lymph nodes (typically 3-5 nodes) from levels III and IV along the lateral internal jugular vein were selectively excised for pathological examination. Therapeutic lateral neck dissection was performed if frozen section pathology confirmed lymph node metastasis.

Observation indicators

Statistical analyses were performed on the baseline characteristics of both the training and internal validation cohorts. Variables included sex, age, surgical method, body mass index (BMI), Hashimoto's thyroiditis, nodular goiter, thyroid adenoma, and preoperative thy-

roid function parameters [free triiodothyronine (FT3), free thyroxine (FT4), total triiodothyronine (TT3), total thyroxine (TT4), thyroid-stimulating hormone (TSH), thyroglobulin (TG), thyroglobulin antibody (TGAb), blood calcium, and parathyroid hormone (PTH)]. Preoperative ultrasound features were recorded, including tumor location, tumor diameter, maximum tumor diameter, invasion, primary lesion characteristics, histological subtype, tumor composition, and morphology.

CN staining characteristics analyzed included the number of positive lymph nodes at levels III and IV, total number of lymph nodes at levels III and IV, number of positive lymph nodes in the lateral neck compartment, total number of lymph nodes in the lateral neck compartment, and metastasis status to levels III and IV lymph nodes.

Based on the presence or absence of LLN metastasis, as confirmed by intraoperative frozen pathology (gold standard), patients in the training cohort were categorized into metastasis and non-metastasis groups for predictive model construction.

Statistical analysis

Statistical analyses were performed using SPSS version 27.0 (IBM Corporation, Armonk, NY) and R version 4.0.4. Graphs were generated using Prism version 10.0 (GraphPad, San Diego, CA). Data normality was assessed using the Shapiro-Wilk test. Quantitative data with normal distributions were expressed as mean ± standard deviation ($\bar{x} \pm sd$) and compared between groups using the independent samples t-test. Non-normally distributed quantitative data were presented as median (Q25, Q75) and compared using the Mann-Whitney U test. Categorical data were expressed as case numbers (percentages) [n (%)] and compared using the chi-squared (χ^2) test.

The least absolute shrinkage and selection operator (LASSO) regression method was employed to identify independent predictors, followed by Cox regression analysis to develop a nomogram prediction model. The validation cohort was used to verify model performance. Receiver operating characteristic (ROC) curve analysis evaluated predictive accuracy, calibration curves assessed model fit, and decision curve analysis (DCA) estimated clinical utility. A *P*-value <0.05 was considered statistically significant.

Results

Comparison of patient demographics and baseline characteristics

The demographic and baseline characteristics of the training and internal validation cohorts are presented in **Table 1**. No statistically significant differences were observed between the two cohorts in age, sex, surgical method, BMI, Hashimoto's thyroiditis, nodular goiter, thyroid adenoma, FT3, FT4, TT3, TT4, TSH, TG, TGAb, serum calcium, or PTH (all P>0.05). Similarly, no significant differences (all P>0.05) were noted for ultrasound features, including tumor location, tumor diameter, maximum tumor diameter, invasion status, primary lesion characteristics, histological subtype, tumor composition, and morphology. Ultrasound images of patients with LLN metastasis are shown in **Figure 3**. Additionally, there were no significant differences (all P>0.05) between the two cohorts regarding the number of lymph nodes at level III, total number of lymph nodes at level IV, number of positive lymph nodes in the lateral neck compartment, total number of lymph nodes in the lateral neck compartment, or metastasis to level III or IV lymph nodes.

Results of univariate Cox regression

The results of the univariate Cox regression analysis for the training cohort are presented in **Table 2**. Factors significantly associated with LLN metastasis included age (HR: 0.866, 95% CI: 0.842-0.891), total thyroidectomy (HR: 0.658, 95% CI: 0.277-1.560), tumors located in the upper pole (HR: 2.610, 95% CI: 1.383-4.926), tumor diameter ≥1 cm (HR: 0.020, 95% CI: 0.006-0.064), maximum tumor diameter (HR: 1.689, 95% CI: 1.430-1.995), regular morphology (HR: 77.989, 95% CI: 19.020-319.778), number of positive lymph nodes in level III (HR: 2.060, 95% CI: 1.664-2.550), number of positive lymph nodes in level IV (HR: 2.040, 95% CI: 1.725-2.413), number of positive lateral cervical lymph nodes (HR: 1.835, 95% CI: 1.645-2.046), metastasis to level III lymph nodes (HR: 0.167, 95% CI: 0.100-0.279), and metastasis to level IV lymph nodes (HR: 0.122, 95% CI: 0.072-0.207)

Table 1. Comparison of patient demographics and baseline characteristics

Characteristics	Training Cohort (N=316)	Internal Test Cohort (N=105)	*t*/*Z*/ χ^2	*P*
Age, y	47.00±11.00	49.00±11.00	1.683	0.094
Sex			0.285	0.594
Female	263 (83.23)	85 (80.95)		
Male	53 (16.77)	20 (19.05)		
BMI, kg/m^2	22.34±2.60	22.18±2.69	0.542	0.588
Surgical method			3.409	0.492
Left lobe resection	96 (30.38)	31 (29.52)		
Left lobe resection + contralateral total lobectomy	19 (6.01)	4 (3.81)		
Right lobe resection	113 (35.76)	43 (40.95)		
Right lobe resection + contralateral total lobectomy	29 (9.18)	5 (4.76)		
Total thyroidectomy	59 (18.67)	22 (20.95)		
Hashimoto's thyroiditis			0.004	0.947
No	267 (84.49)	89 (84.76)		
Yes	49 (15.51)	16 (15.24)		
Nodular goiter			0.724	0.395
No	221 (69.94)	78 (74.29)		
Yes	95 (30.06)	27 (25.71)		
Thyroid adenoma			0.674	0.412
No	315 (99.68)	104 (99.05)		
Yes	1 (0.32)	1 (0.95)		
FT3, pg/mL	3.07±0.54	3.14±0.53	1.009	0.313
FT4, ng/dL	1.29±0.25	1.29±0.28	0.274	0.784
TT3, ng/mL	1.08±0.16	1.08±0.17	0.390	0.697
TT4, μg/dL	7.78 (7.03, 8.69)	7.65 (6.79, 8.35)	1.592	0.111
TSH, μIU/mL	1.48±0.48	1.50±0.55	0.469	0.639
TG, ng/mL	18.50±5.40	18.30±5.20	0.323	0.747
TGAb, IU/mL	15.40 (12.61, 17.30)	15.07 (12.57, 17.09)	0.017	0.986
Blood calcium, mmol/L	2.31±0.15	2.30±0.14	0.743	0.458
PTH, pg/mL	41.74±13.09	39.84±13.36	1.266	0.206
Tumor location			0.199	0.905
Lower pole	119 (37.66)	37 (35.24)		
Middle segment	96 (30.38)	33 (31.43)		
Upper pole	101 (31.96)	35 (33.33)		
Tumor diameter			1.942	0.163
<1 cm	228 (72.15)	83 (79.05)		
≥1 cm	88 (27.85)	22 (20.95)		
Maximum diameter of tumor, cm	0.80 (0.60, 1.08)	0.80 (0.70, 0.90)	0.123	0.902
Tumor laterality			3.962	0.308
Both lobes	58 (18.35)	22 (20.95)		
Isthmus	0 (0.00)	1 (0.95)		
Left lobe	116 (36.71)	33 (31.43)		
Right lobe	142 (44.94)	49 (46.67)		
Invasion			5.602	0.583
Capsule	4 (1.27)	1 (0.95)		
Locally advanced	8 (2.53)	0 (0.00)		
Multiple sites	10 (3.16)	1 (0.95)		
None	259 (81.96)	92 (87.62)		
Peripheral	3 (0.95)	0 (0.00)		
Recurrent laryngeal nerve	4 (1.27)	1 (0.95)		
Strap muscles	28 (8.86)	10 (9.52)		

Primary lesion			1.708	0.191
Multicentric foci	90 (28.48)	37 (35.24)		
Solitary focus	226 (71.52)	68 (64.76)		
Histological subtype			0.015	0.902
Classical	300 (94.94)	100 (95.24)		
Others	16 (5.06)	5 (4.76)		
Tumor Composition			0.373	0.541
Non-solid	52 (16.45)	20 (19.05)		
Solid	264 (83.55)	85 (80.95)		
Morphology			1.546	0.214
Irregular	92 (29.11)	24 (22.86)		
Regular	224 (70.89)	81 (77.14)		
Number of positive lymph nodes in level III	0.00 (0.00, 0.00)	0.00 (0.00, 0.00)	1.195	0.232
Number of positive lymph nodes in level IV	0.00 (0.00, 0.00)	0.00 (0.00, 0.00)	0.110	0.912
Total number of lymph nodes in level III	11.00 (9.00, 14.00)	12.00 (9.00, 15.00)	0.139	0.890
Total number of lymph nodes in level IV	9.00 (8.00, 12.00)	9.00 (7.00, 11.50)	0.210	0.834
Number of positive lymph nodes in the lateral neck compartment	0.00 (0.00, 1.00)	0.00 (0.00, 0.50)	1.213	0.225
Total number of lymph nodes in the lateral neck compartment	22.00 (18.25, 25.00)	22.00 (19.00, 24.00)	0.058	0.954
Metastasis to level III lymph nodes			1.374	0.241
No	265 (83.86)	93 (88.57)		
Yes	51 (16.14)	12 (11.43)		
Metastasis to level IV lymph nodes			0.000	0.990
No	262 (82.91)	87 (82.86)		
Yes	54 (17.09)	18 (17.14)		

Note: BMI: body mass index. FT3: free triiodothyronine. FT4: free thyroxine. TT3: total triiodothyronine. TT4: total thyroxine. TSH: thyroid stimulating hormone. TG: thyroglobulin. TGAb: thyroglobulin antibody. PTH: parathyroid hormone.

Figure 3. Ultrasonogram of a patient with lateral lymph node (LLN) metastasis. Note: Ultrasonogram of a patient with lateral lymph node metastasis, red arrows indicate thyroid nodules.

(all P<0.05). No statistically significant associations were found for the remaining factors (all P>0.05).

Variables selected by LASSO regression for the risk prediction model

Variables with P<0.05 in the univariate Cox regression analysis (age, total thyroidectomy, tumor location in the upper pole, tumor diameter ≥1 cm, maximum tumor diameter, regular morphology, number of positive lymph nodes in levels III and IV, number of positive lateral cervical lymph nodes, and metastasis to levels III and IV lymph nodes) were included in the LASSO regression analysis for further predictor selection. This analysis identified four optimal predictive variables (**Figure 4**), achieving good model fit with maximum parsimony. The selected variables were age, tumor diameter ≥1 cm, regular morphology, and number of positive lateral cervical lymph nodes. Age and the number of positive lateral cervical lymph nodes were natural-log-transformed for model construction. **Figure 5** presents the cross-validated error plot for the LASSO regression model, showing that the most regularized and parsimonious model (within one standard error of the minimum cross-validated error) included these four variables.

Table 2. Results of univariate Cox regression

Characteristics	N	Event N	HR	95% CI	*P*
Age, y	316	58	0.866	0.842-0.891	<0.001
Sex					
Female	263	51	-	-	
Male	53	7	1.308	0.593-2.883	0.506
BMI, kg/m^2	316	58	1.004	0.910-1.107	0.943
Surgical method					
Left lobe resection	96	13	-	-	
Left lobe resection + contralateral total lobectomy	19	7	1.264	0.534-2.993	0.594
Right lobe resection	113	15	0.598	0.247-1.443	0.252
Right lobe resection + contralateral total lobectomy	29	8	1.255	0.454-3.464	0.662
Total thyroidectomy	59	15	0.658	0.277-1.560	0.041
Hashimoto's thyroiditis					
No	267	54	-	-	
Yes	49	4	1.778	0.642-4.927	0.268
Nodular goiter					
No	221	40	-	-	
Yes	95	18	1.094	0.626-1.911	0.753
Thyroid adenoma					
No	315	58	-	-	
Yes	1	0	0.000	0.000-13.890	0.855
FT3, pg/mL	316	58	0.977	0.587-1.625	0.928
FT4, ng/dL	316	58	0.993	0.371-2.663	0.989
TT3, ng/mL	316	58	0.518	0.107-2.495	0.412
TT4, μg/dL	316	58	1.090	0.897-1.326	0.386
TSH, μIU/mL	316	58	0.980	0.559-1.716	0.942
TG, ng/mL	316	58	1.022	0.972-1.074	0.400
TGAb, IU/mL	316	58	1.016	0.947-1.090	0.653
Blood calcium, mmol/L	316	58	0.558	0.096-3.231	0.515
PTH, pg/mL	316	58	0.999	0.980-1.020	0.960
Tumor location					
Lower pole	119	14	-	-	
Middle segment	96	14	1.275	0.607-2.676	0.521
Upper pole	101	30	2.610	1.383-4.926	0.003
Tumor diameter					
<1 cm	228	3	-	-	
≥1 cm	88	55	0.020	0.006-0.064	<0.001
Maximum diameter of tumor, cm	316	58	1.689	1.430-1.995	<0.001
Tumor laterality					
Both lobes	58	14	-	-	
Isthmus	0	0			
Left lobe	116	20	0.607	0.306-1.205	0.154
Right lobe	142	24	0.654	0.338-1.266	0.208
Invasion					
Capsule	4	1	-	-	
Locally advanced	8	1	0.470	0.159-1.390	0.172
Multiple sites	10	5	0.126	0.015-1.088	0.060
None	259	39	0.590	0.080-4.275	0.598
Peripheral	3	1	0.398	0.046-3.426	0.401
Recurrent laryngeal nerve	4	0	1.195	0.137-10.400	0.872
Strap muscles	28	11	1.190	0.150-9.250	0.974

Primary lesion					
Multicentric foci	90	20	-	-	
Solitary focus	226	38	0.703	0.409-1.211	0.204
Histological subtype					
Classical	300	56	-	-	
Others	16	2	2.055	0.501-8.431	0.317
Tumor Composition					
Non-solid	52	10	-	-	
Solid	264	48	1.095	0.552-2.171	0.795
Morphology					
Irregular	92	56	-	-	
Regular	224	2	77.989	19.020-319.778	<0.001
Number of positive lymph nodes in level III	316	58	2.060	1.664-2.550	<0.001
Number of positive lymph nodes in level IV	316	58	2.040	1.725-2.413	<0.001
Total number of lymph nodes in level III	316	58	0.984	0.915-1.059	0.667
Total number of lymph nodes in level IV	316	58	0.920	0.841-1.005	0.064
Number of positive lymph nodes in the lateral neck compartment	316	58	1.835	1.645-2.046	<0.001
Total number of lymph nodes in the lateral neck compartment	316	58	0.965	0.909-1.026	0.257
Metastasis to level III lymph nodes					
No	265	28	-	-	
Yes	51	30	0.167	0.100-0.279	<0.001
Metastasis to level IV lymph nodes					
No	262	23	-	-	
Yes	54	35	0.122	0.072-0.207	<0.001

Comparison of multivariate Cox regression results

Multivariate Cox regression analysis results, presented in **Table 3**, were consistent with the LASSO regression findings. Significant predictive factors included age (HR: 0.944, 95% CI: 0.908-0.982), tumor diameter ≥1 cm (HR: 0.221, 95% CI: 0.053-0.920), regular morphology (HR: 0.090, 95% CI: 0.020-0.470), and number of positive lateral cervical lymph nodes (HR: 0.000, 95% CI: 0.000-0.231) ($P<0.05$). Based on these results, a comprehensive prognostic prediction model was developed. The risk score is calculated as follows:

Risk score = exp[(-0.0577 × ln(age)) + (1.558 × (tumor diameter ≥1 cm)) + (-2.408 × regular morphology) + (0.140 × ln(number of positive lymph nodes in the lateral neck compartment))].

Construction and validation of the LLN metastasis prediction model

Figure 6 presents the prediction model in the form of a nomogram. Age ranges from 15 to 75 years, with a higher risk of LLN metastasis associated with younger age. For every 5-year decrease in age, the risk score increases by approximately 8 points, indicating a negative correlation with the linear predictor. As tumor diameter increases, the risk score also rises. When tumor diameter is ≥1 cm, the estimated risk of metastasis is approximately 40%, demonstrating a positive correlation with the linear predictor. Regarding ultrasound morphology, irregular shapes are associated with higher risk scores for LLN metastasis; under irregular morphology, the incidence of LLN metastasis is around 70%, confirming a positive correlation with the linear predictor. The number of positive lymph nodes in the lateral neck compartment ranges from 1 to 7. For each additional lymph node detected by CN staining, the risk score increases by approximately 3-5 points, showing a positive correlation with the linear predictor.

Figure 7 evaluates the model's performance in both training and internal validation cohorts. In the training cohort (**Figure 7A**), the ROC curve yielded an AUC of 0.911, indicating high predictive accuracy. Similarly, in the internal validation cohort (**Figure 7B**), the ROC analysis

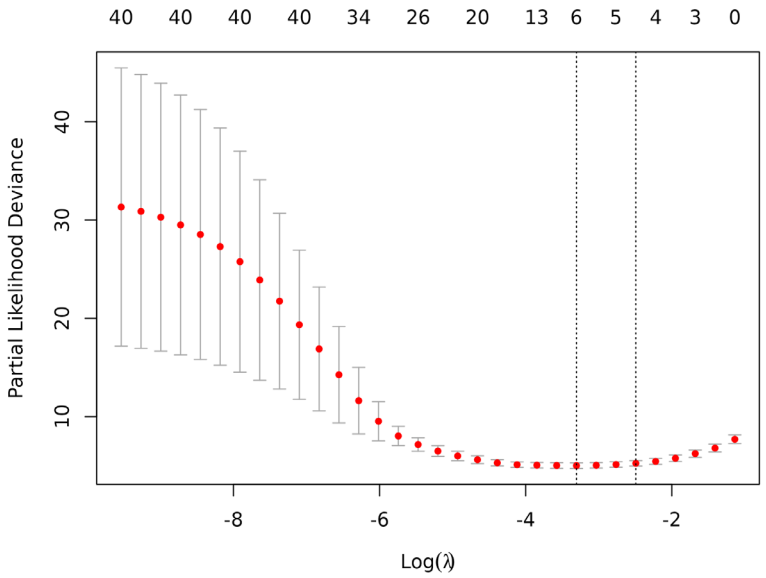

Figure 4. Cross-validation curve of least absolute shrinkage and selection operator (LASSO) regression.

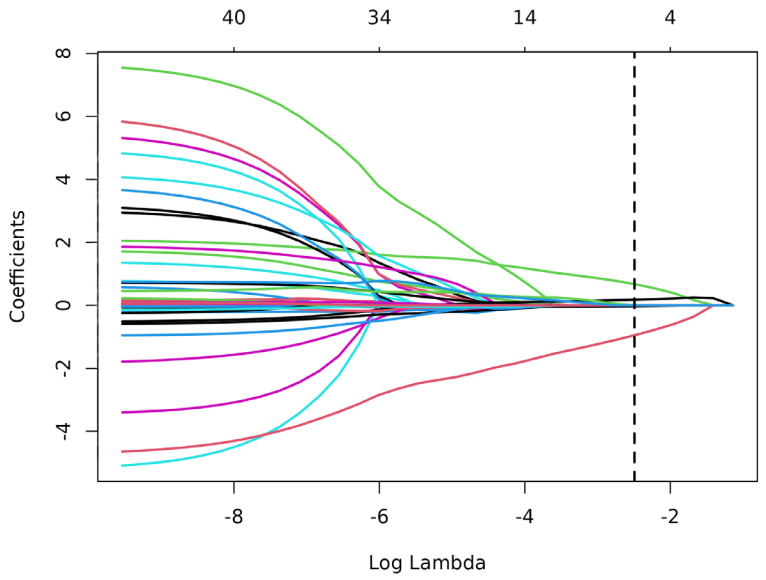

Figure 5. Penalty profiles for variable coefficients.

showed an AUC of 0.916, confirming the model's robust predictive performance.

Figure 8 shows the calibration curves comparing predicted risk (x-axis) with observed risk (y-axis). In the training cohort, the Brier score was 5.70 (95% CI: 4.00-7.40), indicating good predictive accuracy. The ideal calibration line largely coincided with the actual curve, particularly demonstrating excellent fit in the low-risk range (0%-50%). However, greater deviations were observed in the medium-to-high risk ranges. In the internal validation cohort, the Brier score was 4.50 (95% CI: 1.70-7.20), slightly better than that of the training cohort, suggesting more stable performance in the validation set. Overall calibration closely approximated the ideal line, with an excellent fit in the low-risk range (0%-25%), though poorer calibration was noted in medium-to-high risk ranges.

Figure 9 shows the DCA, which plots threshold probability (x-axis, representing the probability of disease progression or metastasis) against net benefit (NB, y-axis). The blue line indicates the net benefit derived from the prognostic model. NB values were largely consistent between the training and validation cohorts, ranging from approximately 0.00 to 0.75.

Clinical validation of factors influencing prognosis

The results of clinical validation, presented in **Table 4**, showed statistically significant differences (all $P<0.05$) between metastatic and non-metastatic patients in age, tumor diameter, morphology, and number of positive lymph nodes in the lateral neck compartment. However, no statistically significant differences (all $P>0.05$) were observed for sex, BMI, surgical approach, Hashimoto's thyroiditis, nodular goiter, thyroid adenoma, FT3, FT4, TT3, TT4, TSH, TG, TGAb, blood calcium, PTH, tumor location, maximum tumor diameter, tumor laterality, invasion, primary lesion characteristics, histological subtype, tumor composition, number of positive lymph nodes in levels III or IV, total number of lymph nodes in levels

Table 3. Results of multivariate Cox regression for the training cohort

Characteristics	N	Event N	HR	95% CI	*P*
Age	316	58	0.944	0.908-0.982	0.004
Tumor diameter					
<1 cm	228	3	-	-	
≥1 cm	88	55	0.221	0.053-0.920	0.038
Morphology					
Irregular	92	56	-	-	
Regular	224	2	0.090	0.020-0.470	0.005
Number of positive lymph nodes in the lateral neck compartment	316	58	0.000	0.000-0.231	<0.001

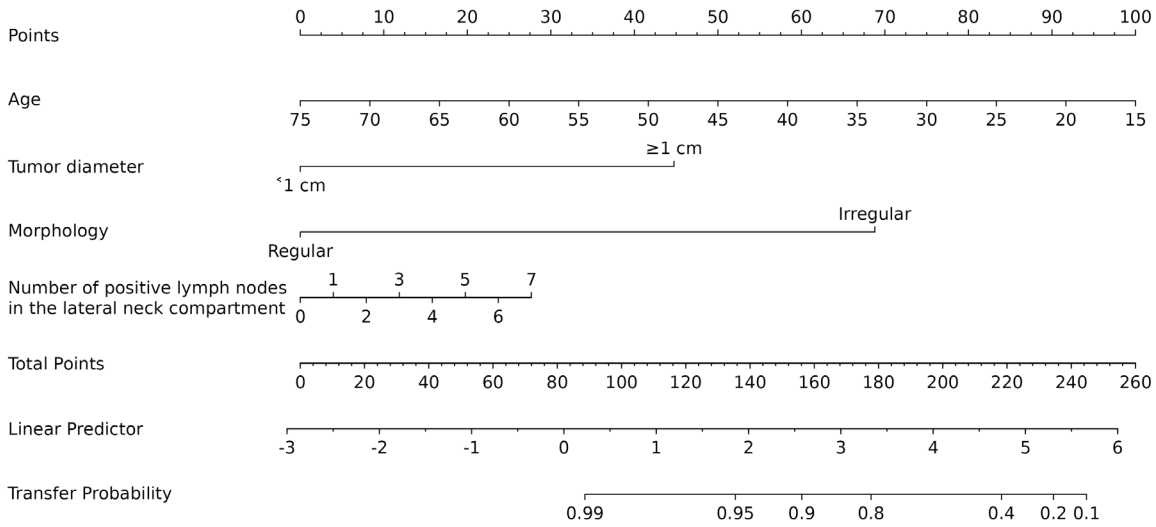

Figure 6. Nomogram for predicting the risk of lateral cervical lymph node (LLN) metastasis in patients with lymph node-negative papillary thyroid carcinoma (PTC). Note: Natural logarithm transformation of age and the number of positive lymph nodes in the lateral neck compartment.

III, IV, or the lateral neck compartment, or metastasis to level III or IV lymph nodes.

Discussion

This study utilized CN tracing technology to develop a prediction model for LLN metastasis in cN0 PTC patients. By constructing a nomogram, we identified age, tumor diameter, tumor morphology, and the number of CN-stained positive lateral cervical lymph nodes as independent predictive factors for LLN metastasis. These findings refine the existing risk assessment system and elucidate the intrinsic relationships between these clinicopathological traits and the biological behavior of LLN metastasis in PTC, providing new evidence to inform clinical decision-making.

Regarding age-related factors, our study observed a significantly increased risk of LLN metastasis in younger patients, consistent with previous research [13]. Several mechanisms may underlie this inverse relationship. At the molecular level, BRAF V600E mutation rates in younger patients' tumors can reach 70-80%, significantly higher than in older patients. This mutation activates the MAPK signaling pathway, promoting epithelial-mesenchymal transition (EMT) and enhancing tumor invasiveness and metastatic potential [14]. From a tumor microenvironment perspective, younger patients exhibit higher lymphatic vessel density (LVD) and vascular endothelial growth factor-C (VEGF-C) expression, creating favorable conditions for LLN metastasis [15]. Recent studies have also revealed distinct immune microenvironment characteristics in younger patients, including a twofold increase in CD8+ T cell exhaustion marker expression, a 30% increase in regulatory T cell (Treg) infiltration, and a 40%

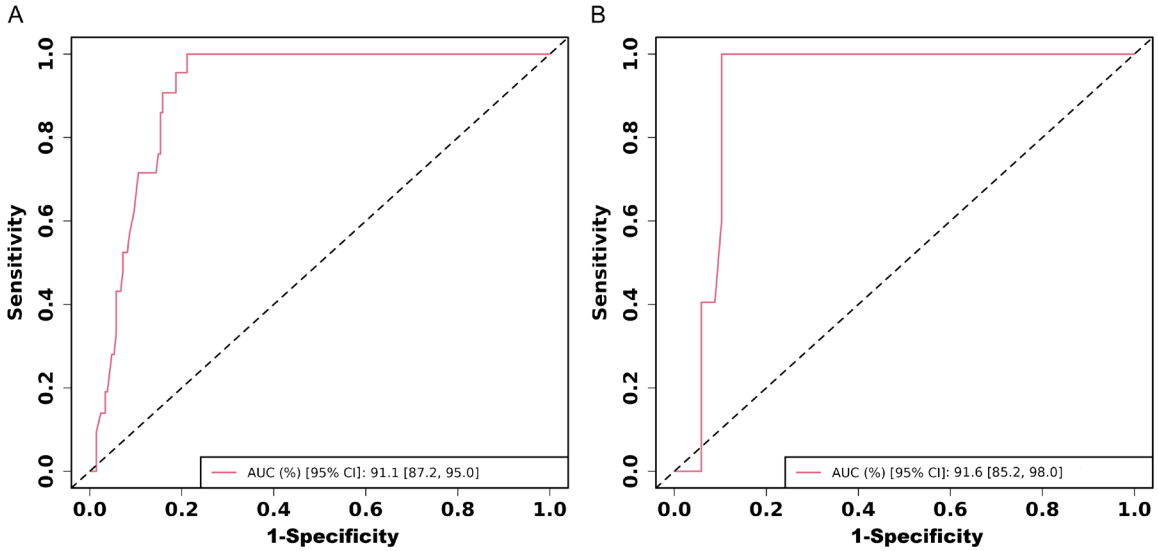

Figure 7. Receiver operating characteristic (ROC) curve of the risk prediction model for lateral cervical lymph node (LLN) metastasis in lymph node-negative papillary thyroid carcinoma (PTC) patients. Note: A: Training cohort receiver operating characteristic (ROC) curve. B: Internal test cohort receiver operating characteristic (ROC) curve.

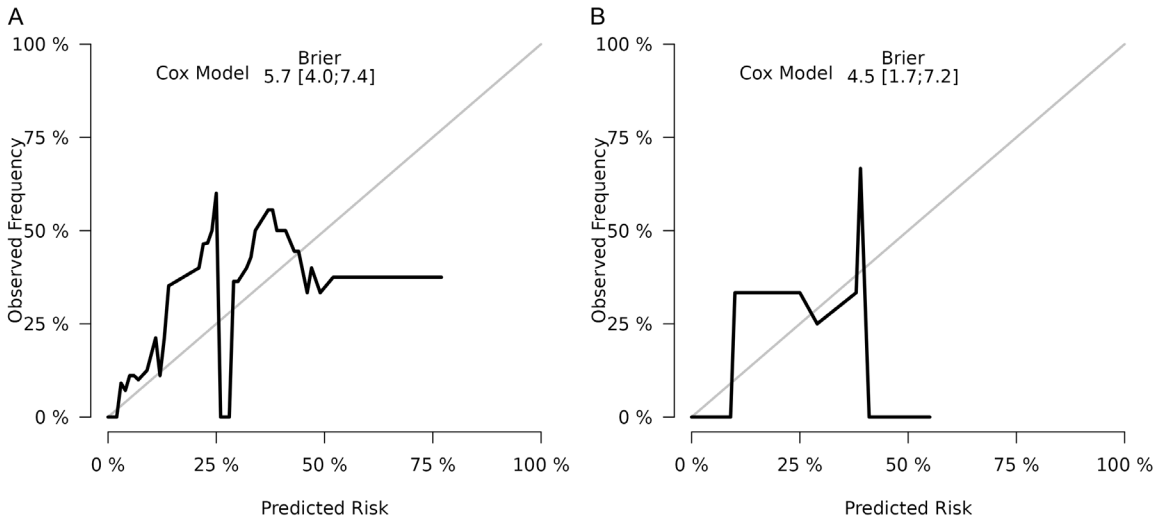

Figure 8. Calibration curve of the risk prediction model for lateral cervical lymph node (LLN) metastasis in lymph node-negative papillary thyroid carcinoma (PTC) patients. Note: A: Training cohort calibration curve. B: Internal test cohort calibration curve.

decrease in dendritic cell maturation [16]. These changes collectively create an immunosuppressive environment that facilitates immune evasion and increases metastatic risk in younger patients.

Building upon previous studies, our research found that a 5-year decrease in age corresponds to an 8-point increase in risk score, providing precise metrics for individualized risk assessment. Tumor diameter, a well-established prognostic indicator, was confirmed to correlate with LLN metastasis in our study [17, 18]. Previous studies have shown that PTCs with diameters ≥1 cm carry a 4.75-fold increased risk of LLN metastasis, consistent with our findings [17]. The underlying mechanisms may involve increased cellular heterogeneity and mechanical pressure as tumor volume increases, leading to basement membrane breakdown and promoting cellular migration [19, 20].

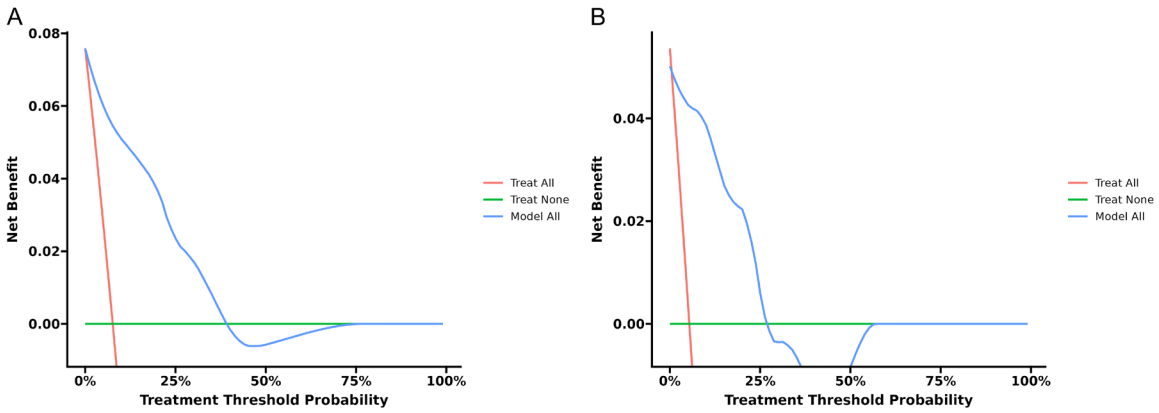

Figure 9. Decision curve analysis (DCA) of the risk prediction model for lateral cervical lymph node (LLN) metastasis in lymph node-negative papillary thyroid carcinoma (PTC) patients. Note: A: Training cohort decision curve analysis (DCA). B: Internal test cohort decision curve analysis (DCA).

Tumor morphological characteristics also demonstrated significant predictive value. This finding deepens our understanding of the morphology - biology correlation in tumors and aligns with previous research [21]. Pathologically, irregular tumor margins typically correspond to invasive growth fronts where tumor cells exhibit enhanced migratory capacity and stromal remodeling activity [22]. Irregular morphology often reflects regions with heightened EMT activity at the tumor-host interface, characterized by downregulated E-cadherin and upregulated vimentin expression, facilitating stromal barrier breach [23]. Radiologically, irregular morphology may indicate heterogeneous intratumoral changes such as fibrosis and calcification, which are closely associated with clonal selection under tumor evolutionary pressures [24].

The application of CN tracing technology in this study represents a significant advancement. Compared to traditional imaging modalities, this method improves sensitivity by 30-40%, enabling detection of micrometastases smaller than 2 mm in diameter [25]. Our results provide a quantitative assessment of nodal involvement, demonstrating that metastatic risk increases by approximately 15% with each additional positive lymph node. This improved predictive performance is likely attributable to the inherent diagnostic accuracy of CN tracing as an intraoperative detection method, which has shown high concordance with pathological findings from lateral neck dissection specimens [26].

From a translational medicine perspective, CN tracing serves not merely as a diagnostic tool; the lymphatic network remodeling patterns it reveals may also reflect systemic alterations within the tumor microenvironment [27]. This novel insight opens new avenues for researching metastasis mechanisms.

The clinical validation results presented in **Table 4** further confirm the reliability of the prognostic model, demonstrating that younger age, tumor diameter ≥1 cm, irregular morphology, and a higher number of CN-stained positive lateral cervical lymph nodes were all significantly associated with metastasis. These findings are highly consistent with the independent predictive factors identified during model construction.

Compared with existing studies, our research not only validates the negative prognostic impact of younger age and larger tumor diameter - aligning with the findings of Zhang et al. [28] - plus it also quantifies the predictive value of lymph node involvement through CN technology, thereby addressing the limitations of conventional imaging in detecting micrometastases. Furthermore, the strong association between irregular tumor morphology and metastasis supports the “invasive margin growth” theory proposed by Seong et al., with potential mechanisms involving enhanced EMT and stromal remodeling activity in tumor cells [29].

From a clinical perspective, the risk of metastasis increases by approximately 15% with each

Table 4. Clinical validation of factors influencing prognosis

Characteristics	Metastatic group (N=22)	Non-metastatic group (N=79)	$t/Z/\chi^2$	*P*
Age, y	32.45±8.04	49.23±8.69	8.133	<0.001
Sex			0.069	0.793
Female	11 (50.00)	42 (53.16)		
Male	11 (50.00)	37 (46.84)		
BMI, kg/m^2	22.52±3.47	23.00±2.36	0.741	0.460
Surgical method			0.578	0.966
Left lobe resection	5 (22.73)	16 (20.25)		
Left lobe resection + contralateral total lobectomy	1 (4.55)	4 (5.06)		
Right lobe resection	11 (50.00)	44 (55.70)		
Right lobe resection + contralateral total lobectomy	2 (9.09)	8 (10.13)		
Total thyroidectomy	3 (13.64)	7 (8.86)		
Hashimoto's thyroiditis			0.205	0.651
No	19 (86.36)	65 (82.28)		
Yes	3 (13.64)	14 (17.72)		
Nodular goiter			0.961	0.327
No	20 (90.91)	65 (82.28)		
Yes	2 (9.09)	14 (17.72)		
Thyroid adenoma			2.978	0.084
No	18 (81.82)	74 (93.67)		
Yes	4 (18.18)	5 (6.33)		
FT3, pg/mL	3.07 (2.83, 3.65)	3.27 (2.90, 3.63)	0.843	0.399
FT4, ng/dL	1.22±0.28	1.28±0.27	0.878	0.382
TT3, ng/mL	1.12±0.21	1.08±0.15	0.869	0.387
TT4, μg/dL	7.45±1.55	7.39±1.21	0.581	0.848
TSH, μIU/mL	1.57±0.62	1.69±0.58	0.477	0.404
TG, ng/mL	18.95±3.63	18.20±4.89	0.671	0.504
TGAb, IU/mL	16.08±2.63	15.63±2.69	0.688	0.493
Blood calcium, mmol/L	2.25±0.19	2.27±0.14	0.515	0.608
PTH, pg/mL	35.94 (24.46, 46.36)	42.17 (31.31, 48.24)	1.728	0.084
Tumor location			0.195	0.907
Lower pole	8 (36.36)	31 (39.24)		
Middle segment	8 (36.36)	30 (37.97)		
Upper pole	6 (27.27)	18 (22.78)		
Tumor diameter			22.060	<0.001
<1 cm	3 (13.64)	55 (69.62)		
≥1 cm	19 (86.37)	24 (30.38)		
Maximum diameter of tumor, cm	1.10 (1.00, 1.23)	0.90 (0.80, 1.90)	1.945	0.052
Tumor laterality			2.872	0.412
Both lobes	5 (22.73)	8 (10.13)		
Isthmus	1 (4.55)	2 (2.53)		
Left lobe	9 (40.91)	36 (45.57)		
Right lobe	7 (31.82)	33 (41.77)		
Invasion			3.579	0.733
Capsule	2 (9.09)	5 (6.33)		
Locally advanced	0 (0.00)	1 (1.27)		
Multiple sites	3 (13.64)	8 (10.13)		
None	12 (54.55)	46 (58.23)		
Peripheral	2 (9.09)	2 (2.53)		
Recurrent laryngeal nerve	3 (13.64)	14 (17.72)		
Strap muscles	0 (0.00)	3 (3.80)		

Primary lesion			0.440	0.507
Multicentric foci	4 (18.18)	10 (12.66)		
Solitary focus	18 (81.82)	69 (87.34)		
Histological subtype			2.557	0.110
Classical	15 (68.18)	66 (83.54)		
Others	7 (31.82)	13 (16.46)		
Tumor Composition			0.698	0.403
Non-solid	5 (22.73)	12 (15.19)		
Solid	17 (77.27)	67 (84.81)		
Morphology			21.891	<0.001
Irregular	16 (72.73)	16 (20.25)		
Regular	6 (27.27)	63 (79.75)		
Number of positive lymph nodes in level III	0.00 (0.00, 0.00)	0.00 (0.00, 1.00)	1.770	0.077
Number of positive lymph nodes in level IV	0.50 (0.00, 2.00)	0.00 (0.00, 1.00)	1.864	0.062
Total number of lymph nodes in level III	10.00 (7.00, 14.00)	12.00 (8.00, 15.00)	0.623	0.533
Total number of lymph nodes in level IV	8.00 (6.75, 9.00)	8.00 (5.00, 12.00)	0.534	0.594
Number of positive lymph nodes in the lateral neck compartment	5.00 (3.75, 8.00)	0.00 (0.00, 1.00)	6.637	<0.001
Total number of lymph nodes in the lateral neck compartment	20.36±5.61	21.92±7.56	0.900	0.370
Metastasis to level III lymph nodes			1.260	0.262
No	19 (86.36)	74 (93.67)		
Yes	3 (13.64)	5 (6.33)		
Metastasis to level IV lymph nodes			1.380	0.240
No	17 (77.27)	69 (87.34)		
Yes	5 (22.73)	10 (12.66)		

Note: BMI: body mass index. FT3: free triiodothyronine. FT4: free thyroxine. TT3: total triiodothyronine. TT4: total thyroxine. TSH: thyroid stimulating hormone. TG: thyroglobulin. TGAb: thyroglobulin antibody. PTH: parathyroid hormone.

additional positive lymph node in the lateral neck compartment. This highlights the critical role of the lymphatic system as a metastatic pathway and is consistent with Zhou et al.'s research on lymph node microenvironment remodeling [30]. Overall, these results validate the clinical applicability of the model and elucidate the mechanistic relevance of its predictive factors: age reflects host immune surveillance capacity; tumor diameter and morphology indicate invasive potential; and the number of CN-marked lymph nodes visually represents metastatic burden [31]. Thus, this model integrates multidimensional biological features, providing a robust foundation for individualized surgical decision-making.

Despite these significant advances, several limitations warrant consideration. Although the retrospective design ensured data completeness, it may have introduced selection bias, particularly regarding the representation of specific patient subgroups. While the sample size met statistical requirements, analysis of certain rare histological variants was underpowered. Additionally, although CN tracing enhanced detection sensitivity, optimizing its visualization for anatomically obscured regions such as level IIb lymph nodes remains necessary.

Future investigations will focus on conducting multicenter randomized controlled trials to validate the generalizability of this predictive model, while exploring the synergistic value of integrating CN tracing with advanced imaging modalities, including ultrasound elastography and CT perfusion. These research directions hold substantial scientific merit and promise meaningful improvements in clinical practice.

In conclusion, this CN-guided nomogram is a practical and highly accurate tool for intraoperative risk stratification of LLN metastasis in cN0 PTC patients. By integrating tracer-based lymph node assessment with conventional clinicopathological factors, the model offers superior predictive capability compared to existing methods. This approach could potentially reduce unnecessary neck dissections while ensuring appropriate management of high-risk cases. Multicenter validation and

incorporation of molecular markers are important next steps toward clinical implementation.

Disclosure of conflict of interest

The authors declare that they have no known competing financial interests or personal relationships that could have appeared to influence the work reported in this paper.

Address correspondence to: Hongshen Chen, Department of Breast and Thyroid Surgery, Affiliated Zhongshan Hospital of Dalian University, Dalian 116001, Liaoning, The People's Republic of China. Tel: +86-15566828088; E-mail: dl_chs020523@163.com

References

[1] Tian W, Su X, Hu C, Chen D and Li P. Ferroptosis in thyroid cancer: mechanisms, current status, and treatment. Front Oncol 2025; 15: 1495617.

[2] Ryu YJ, Kwon SY, Lim SY, Na YM and Park MH. Predictive factors for skip lymph node metastasis and their implication on recurrence in papillary thyroid carcinoma. Biomedicines 2022; 10: 179.

[3] Guo Y, Liu Y, Teng W, Pan Y, Zhang L, Feng D, Wu J, Ma W, Wang J, Xu J, Zheng C, Zhu X, Tan Z and Jiang L. Predictive risk-scoring model for lateral lymph node metastasis in papillary thyroid carcinoma. Sci Rep 2025; 15: 9542.

[4] Du J, Yang Q, Sun Y, Shi P, Xu H, Chen X, Dong T, Shi W, Wang Y, Song Z, Shang X and Tian X. Risk factors for central lymph node metastasis in patients with papillary thyroid carcinoma: a retrospective study. Front Endocrinol (Lausanne) 2023; 14: 1288527.

[5] Taniuchi M, Kawata R, Terada T, Higashino M, Aihara T and Jinnin T. Central node dissection from the perspective of lateral neck node metastasis in papillary thyroid carcinoma. Auris Nasus Larynx 2024; 51: 266-270.

[6] Song WJ, Um IC, Kwon SR, Lee JH, Lim HW, Jeong YU, Chung SM, Moon JS, Yoon JS, Won KC and Lee HW. Predictive factors of lymph node metastasis in papillary thyroid cancer. PLoS One 2023; 18: e0294594.

[7] Liu WQ, Yang JY, Wang XH, Cai W and Li F. Analysis of factors influencing cervical lymph node metastasis of papillary thyroid carcinoma at each lateral level. BMC Surg 2022; 22: 228.

[8] Pham MC, Nguyen T and Nguyen HP. Surgical complications in papillary thyroid cancer patients with cervical lymph node metastases. Clin Med Insights Oncol 2024; 18: 11795549241233692.

[9] Ding H, Xu F, Guan W and Sang J. Correlation between body mass index and lymph node metastasis in papillary thyroid carcinoma: a retrospective clinical study. Gland Surg 2024; 13: 1400-1407.

[10] Zhang W, Shu Y, Ni D, Wan Z and Yang S. Comparison of two suspension injection tracers of nano activated carbon and methylene blue in mapping and tracing of sentinel lymph nodes of patients with endometrial cancer. Pak J Med Sci 2022; 38: 1601-1605.

[11] Lim JH, Han A, Cho SJ, Hahn S and Kim SG. Nomogram prediction for gastric cancer development. Clin Transl Gastroenterol 2025; 16: e00833.

[12] Gordon AJ, Dublin JC, Patel E, Papazian M, Chow MS, Persky MJ, Jacobson AS, Patel KN, Suh I, Morris LGT and Givi B. American thyroid association guidelines and national trends in management of papillary thyroid carcinoma. JAMA Otolaryngol Head Neck Surg 2022; 148: 1156-1163.

[13] Ma T, Zhang S, Huang D, Zhang G, Chen B and Zhang N. Endoscopic-assisted lateral neck dissection and open lateral neck dissection in the treatment of lateral neck lymph node metastasis in papillary thyroid carcinoma: a comparison of therapeutic effect. Pak J Med Sci 2022; 38: 1905-1910.

[14] Li X, Duan Y, Liu D, Liu H, Zhou M, Yue K, Shuai Y, Wang Y, Ji C, Jing C, Wu Y and Wang X. Diagnostic model incorporating clinicopathological characteristics of delphian lymph node metastasis risk profiles in papillary thyroid cancer. Front Endocrinol (Lausanne) 2021; 12: 591015.

[15] Luo X, Zhou Y, Rao K, Xiang J, Ning S, Zhu D, Li G and Chen H. Biomimetic cascade nanozyme catalytic system for the treatment of lymph node metastasis in gastric cancer. Small 2025; 21: e2411576.

[16] Wang Y, Deng C, Shu X, Yu P, Wang H, Su X and Tan J. Risk factors and a prediction model of lateral lymph node metastasis in CN0 papillary thyroid carcinoma patients with 1-2 central lymph node metastases. Front Endocrinol (Lausanne) 2021; 12: 716728.

[17] Liu C, Zhang L, Liu Y, Zhao Q, Pan Y and Zhang Y. Value of pyruvate carboxylase in thyroid fine-needle aspiration wash-out fluid for predicting papillary thyroid cancer lymph node metastasis. Front Oncol 2021; 11: 643416.

[18] Zhang J, Jia G, Su Y, Zhang Z, Xiong H, Xu Q and Meng S. Prediction of cervical lymph nodes metastasis in Papillary Thyroid Carcinoma (PTC) Using Nodal Staging Score (NSS). J Oncol 2022; 2022: 9351911.

[19] Chmiel P, Krotewicz M, Szumera-Ciećkiewicz A, Bartnik E, Czarnecka AM and Rutkowski P. Re-

view on lymph node metastases, sentinel lymph node biopsy, and lymphadenectomy in sarcoma. Curr Oncol 2024; 31: 307-323.
[20] Qiu P, Guo Q, Pan K and Lin J. Development of a nomogram for prediction of central lymph node metastasis of papillary thyroid microcarcinoma. BMC Cancer 2024; 24: 235.
[21] Shen W, Pan XJ and Li QH. Utility and significance of clinical risk factor scoring model in predicting central compartment lymph node metastasis (CLNM) in patients with papillary thyroid cancer (PTC). Pak J Med Sci 2022; 38: 214-218.
[22] Liu Q, Li Y, Hao Y, Fan W, Liu J, Li T and Liu L. Multi-modal ultrasound multistage classification of PTC cervical lymph node metastasis via DualSwinThyroid. Front Oncol 2024; 14: 1349388.
[23] Tu CL and Lin CH. Metastasis of pulmonary adenocarcinoma to the thyroid closely mimics papillary thyroid carcinoma. Kaohsiung J Med Sci 2021; 37: 831-832.
[24] Wang Z, Wang H, Zhou Y, Li L, Lyu M, Wu C, He T, Tan L, Zhu Y, Guo T, Wu H, Zhang H and Sun Y. An individualized protein-based prognostic model to stratify pediatric patients with papillary thyroid carcinoma. Nat Commun 2024; 15: 3560.
[25] Yu W, Xu G, Sun J and Zhong N. Carbon nanoparticles guide contralateral central neck dissection in patients with papillary thyroid cancer. Oncol Lett 2018; 16: 447-452.
[26] Wei R, Zhuang Y, Wang L, Sun X, Dai Z, Ge Y, Wang H and Song B. Histogram-based analysis of diffusion-weighted imaging for predicting aggressiveness in papillary thyroid carcinoma. BMC Med Imaging 2022; 22: 188.
[27] Dou Y, Hu D, Chen Y, Xiong W, Xiao Q and Su X. PTC located in the upper pole is more prone to lateral lymph node metastasis and skip metastasis. World J Surg Oncol 2020; 18: 188.
[28] Zhang C, Li BJ, Liu Z, Wang LL and Cheng W. Predicting the factors associated with central lymph node metastasis in clinical node-negative (cN0) papillary thyroid microcarcinoma. Eur Arch Otorhinolaryngol 2020; 277: 1191-1198.
[29] Seong CY, Chai YJ, Lee SM, Kim SJ, Choi JY, Lee KE, Hwang KT, Park SW and Yi KH. Significance of distance between tumor and thyroid capsule as an indicator for central lymph node metastasis in clinically node negative papillary thyroid carcinoma patients. PLoS One 2018; 13: e0200166.
[30] Zhou LQ, Zeng SE, Xu JW, Lv WZ, Mei D, Tu JJ, Jiang F, Cui XW and Dietrich CF. Deep learning predicts cervical lymph node metastasis in clinically node-negative papillary thyroid carcinoma. Insights Imaging 2023; 14: 222.
[31] Xue S, Zhang L, Pang R, Wang P, Jin M, Guo L, Zhou Y, Dong B and Chen G. Predictive factors of central-compartment lymph node metastasis for clinical N0 papillary thyroid carcinoma with strap muscle invasion. Front Endocrinol (Lausanne) 2020; 11: 511.